A Purely Green Synthesis of Silver Nanoparticles using *Carica papaya*, *Manihot esculenta*, and *Morinda citrifolia*: Synthesis and Antibacterial Evaluations

Achmad Syafiuddin[1], Salmiati[1,2*], Tony Hadibarata[3], Mohd Razman Salim[1,2], Ahmad Beng Hong Kueh[4]

[1]Department of Environmental Engineering, Faculty of Civil Engineering,
Universiti Teknologi Malaysia, 81310 UTM Johor Bahru, Johor, Malaysia

[2]Centre for Environmental Sustainability and Water Security (IPASA), Research Institute for Sustainable Environment, Faculty of Civil Engineering, Universiti Teknologi Malaysia, 81310 UTM Johor Bahru, Johor, Malaysia

[3]Department of Environmental Engineering, Faculty of Engineering and Science, Curtin University, 98009 Miri, Sarawak, Malaysia

[4]Construction Research Centre (CRC), Institute for Smart Infrastructure and Innovative Construction (ISIIC), Faculty of Civil Engineering, Universiti Teknologi Malaysia,
81310 UTM Johor Bahru, Johor, Malaysia

[*]*Corresponding author: salmiati@utm.my*

[*]*Current address:* Center for Environmental Sustainability and Water Security (IPASA), Universiti Teknologi Malaysia, 81310 UTM Johor Bahru, Johor, Malaysia

Tel.: +607-5531579; Fax: +607-5531575

Abstract

Green procedure for synthesizing silver nanoparticles (AgNPs) is currently considered due to its economy and toxic-free effects. Several existing works on synthesizing AgNPs using leaves extract still involve the use of physical or mechanical treatment such as heating or stirring, which consume a lot of energy. To extend and explore the green extraction philosophy, we report here the synthesis and antibacterial evaluations of a purely green procedure to synthesize AgNPs using *Carica papaya, Manihot esculenta,* and *Morinda citrifolia* leaves extract without the aforementioned additional treatment. The produced AgNPs were characterized using the ultraviolet–visible spectroscopy (UV-vis), field emission scanning electron microscopy (FESEM), energy-dispersive X-ray spectroscopy (EDX), Fourier transform infrared spectroscopy (FTIR), and antibacterial investigations. For antibacterial tests, two bacteria namely *Escherichia Coli* and *Bacillus Cereus* were selected. The presently employed method has successfully produced spherical AgNPs having sizes ranging from 9 to 69 nm, with plasmonic characteristics ranging from 356 to 485 nm, and energy-dispersive X-ray peak at

approximately 3 keV. In addition, the smallest particles can be produced when *Manihot esculenta* leaves extract was applied. Moreover, this study also confirmed that both the leaves and synthesized AgNPs exhibit the antibacterial capability, depending on their concentration and the bacteria type.

Keywords: *Carica papaya*, *Manihot esculenta*, *Morinda citrifolia*, green synthesis, silver nanoparticles

Introduction

Silver nanoparticles (AgNPs) have been the attraction for various active research subjects in recent years due to their appealing electrical [1], optical [2, 3], physical [4], and thermal behaviors [5]. Their applications are widely found in the biological products [6], photovoltaics [7], catalysts [8], and chemical sensors [9]. Of interest also are their utilization in fabrics [10], antimicrobial coatings [6, 11], biomedical devices [12, 13], and wound dressing owing to their bacterial-repelling property [14, 15]. It is well known that their properties depend strongly on their sizes, species, shapes, and procedures of the synthesis.

Studies on the toxicity properties of AgNPs on the bacterial growth have been well-documented in the literature. Colony forming unit (CFU) and inhibition zone are common approaches used to investigate their antibacterial capability. It is established that the nanoparticles have a large surface area compared to micro or macroparticles. Thus, nanoparticles have a higher tendency of interaction with the bacterial cells compared to the bigger particles. AgNPs with the size of 5 nm demonstrated the greatest antibacterial capability against *Escherichia coli* (*E. coli*) MTCC 443 and *Staphylococcus aureus* NCIM 5201 compared to the larger particles such as 7 nm and 10 nm sizes at similar bacterial concentrations [16]. Another study also found that smaller AgNPs with the sizes ranging from 15 to 50 nm exhibited more antibacterial activity than larger particles ranging from 25 to 70 nm, 30 to 80 nm, and 30 to 200 nm against *Pseudomonas aeruginosa* and *E. coli*. In addition, the shape of AgNPs also affected their antibacterial capability [17]. The minimum inhibitory concentration of AgNPs in other shapes such as nanocubes, nanospheres, and nanowires were found to be 37.5, 75, and 100 μg mL^{-1} when a bacterial concentration of 10^4 CFU mL^{-1} was employed. The high antibacterial activity of these anisotropic-shaped AgNPs was due to the basal plane with high-atom-density facets acting as the maximum reactivity sites [17].

Since AgNPs are proven to be toxic, their existence and applications in the environment have become a hot topic for research [18-23]. The presence of AgNPs in the environment is commonly attributed to their release from commercial products. For instance, about 5 to 95% of the total amount of AgNPs in the consumer

products were expelled to sewage treatment plants. In addition, they were released from six types of socks containing AgNPs with the concentrations ranging from 1.5 to 650 μg in 500 mL of the wash water [24]. Shirts, medical masks and cloths, toothpaste, shampoo, detergent, towels, teddy bear toys, and two humidifiers were also found to release AgNPs to the wash water with the concentration of about 45 μg $product^{-1}$ [25]. Furthermore, about 85 g d^{-1} of AgNPs were discharged from the laundry into the sewer system and the municipal wastewater treatment plant [26]. It is of importance to note that AgNPs in the environment can be transformed into different forms, such as ionic Ag, Ag_2O, and Ag_2S depending on the environmental conditions via physical and chemical events [27].

There exist many works on synthesizing and characterizing numerous properties of AgNPs in the past several years [28-34]. Since understanding how their various properties change corresponding to different extracting techniques is vital to achieve their most desirable performance, several production approaches were continually proposed and revised. Although many extracting methods are possible, the current trend focuses on how this can be carried out in a cheaper and greener manner. Currently, synthesis of AgNPs using plant extracts is highly considered because of their simplicity, abundant availability, and potential to eliminate a complicated preparation such as the use of microorganism as presented by Mishra et al. [34]. The use of leaves, seeds, roots, and fruits in the green synthesis of AgNPs have been continually proposed and remain an active subject for research investigation. Among these, the exploration of leaves extract as the reducing and stabilizing agent to synthesize nanoparticles of AgNPs is a preferable approach due to their wide obtainability in the environment. Table 1 lists the recent pattern of AgNPs synthesis using numerous leaf extracting approaches [4, 31, 32, 35-41]. Several works, for instance Salem et al. [40], Vijay Kumar et al. [41], Muthukrishnan et al. [38], and He et al. [33], on the production of AgNPs still employed physical or mechanical treatments such as heating or stirring, which consume a lot of energy.

Therefore, the aim of the present study is to evaluate the suitability of the use of *Carica papaya* (*C. papaya*), *Manihot esculenta* (*M. esculenta*), and *Morinda citrifolia* (*M. citrifolia*) leaves extract without the aforementioned additional treatment to synthesize AgNPs. It is essential to provide a purely green procedure for future exploration to minimize the use of energy, its massive consumption of which is evidenced in other alternative approaches. *C. papaya* is a climacteric tropical plant originated from the Southern Mexico. It is also generally well-populated in the tropical climate such as Brazil, Malaysia, and Indonesia. In addition, *M. esculenta,* generally known as Cassava, is well recognized as a carbohydrate source. In the tropical region, it is the third largest source of carbohydrates after rice and maize [42]. Furthermore, *M. citrifolia* is a medical plant

that is widely grown in Malaysia and Indonesia. In these countries, it is well known as Mengkudu widely explored for numerous medical applications. Leaves of these plants are commonly utilized as a vegetable source as well [43, 44]. For comprehensive details, the chemical compositions of these three types of leaf are offered in Table 2 [42, 45-48]. Many existing works have confirmed that the biomolecules contained in leaves such as proteins, enzymes, polysaccharides, amino acids, and vitamins can act as bioreductant from reducing metal ions to the formation of AgNPs in the solution [49, 50]. The use of all currently proposed leaves is due to their possession of these favorable properties as presented in Table 2. Also, since previous studies have proven that these leaves have antibacterial capability, their exploration either as extract or capping on AgNPs are interesting for further research pursuit. Such study can be highly beneficial for future medical applications.

Materials and Methods

Materials

The basic compound under study, silver nitrate ($AgNO_3$, QReC, Auckland, New Zealand), was used as the silver salt. *C. papaya, M. esculenta,* and *M. citrifolia* leaves were collected from the surrounding area of Universiti Teknologi Malaysia, Johor Bahru, Malaysia. 0.45 μm nylon membrane (Whatman® Nylon membrane, Sigma-Aldrich, St. Louis, MO, USA) was used as the filter. For synthesizing process, solutions were prepared using the ultrapure water (resistivity 18.2 MΩ cm) (Arium Ultrapure Water System, Sartorius Malaysia Sdn Bhd, Kuala Lumpur, Malaysia). Bacteria, *E. coli* and *Bacillus cereus* (*B. cereus*), were obtained from the Faculty of Biosciences and Medical Engineering, Universiti Teknologi Malaysia. In addition, agar powder (OXOID CM0003, Oxoid Ltd, Cheshire, England) was used. Broth powder (Merck VM447243, Merck KGaA, Darmstadt, Germany) was also employed in this study.

Preparation of leaves extract

To remove impurities, fresh leaves were first washed using the tap water and followed by the ultrapure water three times each. Then, 10 g of leaf was mixed with 300 mL ultrapure water in a 500 mL Erlenmeyer flask. The mixture was heated to 250 °C for 30 min, before cooled at the room temperature. To obtain a pure leaves extract, the mixture was then filtered through a nylon membrane filter of 0.45 μm . The solution passing the membrane was then stored in a fridge at a temperature of 7 °C for future use. The same extraction procedure was then applied for all proposed leaves.

Synthesis of AgNPs

Firstly, $AgNO_3$ solution (100 mL in volume) was prepared using $AgNO_3$ and the ultrapure water with a concentration of 0.15 M in a 500 mL Erlenmeyer flask. To initiate the synthesis process, 100 mL leaves extract was added slowly into the $AgNO_3$ solution. The mixtures were then left overnight to perform the reduction of metal ions to the formation of AgNPs in the solution. For control, a 100 mL $AgNO_3$ solution with the same concentration without leaves extract was also prepared. For AgNPs harvesting, the mixtures were then centrifuged at $8000\times g$ for 45 min and the pellet obtained in this process was collected. To purify AgNPs production, the pellet was then cleansed with the ultrapure water before centrifuged at $8000\times g$ for 45 min. The purification process was repeated for three times. Next, the pellet was air dried. AgNPs obtained using this procedure were then stored for the characterization. The same procedure was carried out for synthesizing AgNPs using other leaves extract.

Plasmonic investigation

Plasmonic property of AgNPs was characterized using the UV-Vis spectrometer (Perkin–Elmer, No. 101N4110104) installed with the Lambda 25 software. It was operated at a resolution of 1 nm, a scan speed of 960 nm min^{-1}, and the electromagnetic wavelength in the range of 300 to 700 nm. 2 mL sample mixtures were injected into the UV-vis tube. In this inspection, the ultrapure water was used as a blank.

FTIR characterization

For this observation, AgNPs were mixed with potassium bromide (1:100) to produce the specimen in a pellet form. The pellet was pressed hydraulically (Specac model with a serial number of N29850) at 10 tons in pressure. The pressed pellet was then taken and placed into the FTIR holder. Biomolecules bonding of the synthesized AgNPs was identified using the FTIR spectrometer (PerkinElmer Frontier-GPOB model 96046) installed with the PerkinElmer Spectrum software. The spectrometer used OptKBr (7800 to 400 cm^{-1}) as beam splitter and MIR TGS (15000 to 370 cm^{-1}) as detector. This characterization was conducted using a spectrum wavelength in the range of 650 to 4000 cm^{-1} at a resolution of 4 cm^{-1} and accumulations of 10 scans at room temperature.

FESEM and SEM-EDX

AgNPs morphologies were also characterized by means of the field emission scanning electron microscopy (FESEM ZEISS Supra 35VP). This apparatus was supplied by Carl Zeiss Sdn Bhd. It was operated at an accelerating of 5 kV with a magnification of 50000×. AgNPs elements were then confirmed by SEM-EDX (HITACHI S-3400N) equipped with the Bruker Quantax software. It was operated at a voltage of 15 kV.

Preparation of agar and broth nutrients

To produce agar nutrient, 14 g of the nutrient agar powder was mixed with 500 mL of ultrapure water. In addition, 4 g of the broth powder was prepared with the same water mixture to produce the broth nutrient solution. In the preparation, all solutions were sterilized using the autoclave ALP (model CL-40M no.805415) at a temperature of 121 ^{o}C for 2 h.

Colony forming test

Colony forming test was prepared using the previous study by Mueller and Hinton [51] as basis. $AgNO_3$ and leaves extract were freshly prepared and mixed for this test. A 10-mL $AgNO_3$ solution (0.15 M) was prepared using the ultrapure water in a 50 mL plastic tube. A variation in the leaf quantity was made such that ratios of 5:2 and 5:3 for $AgNO_3$ and leaves extract were obtained. $AgNO_3$ solution with the same concentration was also prepared as a control case. Bacterial cultures of about 5×10^{15} colony were taken and about 0.1 mL of inoculum was mixed with the solution and incubated at 37 ^{o}C for 24 h. For comparison purpose, the pure leaves extract was also studied. Then, the colony of the survived bacteria was counted. This test procedure was carried out for all considered leaves.

Inhibition zone test

In this investigation, antibacterial activity was determined by using the paper disk assay method as basis [52]. In this test, $AgNO_3$ and leaves extract were freshly prepared and mixed analogously to the method employed in the colony forming test. Bacterial cultures of about 5×10^{15} colony were taken and about 0.1 mL of inoculum was spread on each agar plate. Filter paper (2 mm in diameter) was steeped in AgNPs solution with the similar variation as the colony forming test for 1 min and then put onto the agar plate. As comparison, the filter paper was also steeped in $AgNO_3$ solution. Next, the plate was incubated at 37 ^{o}C for 24 h. An inhibition zone can be described as the clear area surrounding the filter paper containing AgNP solution deposited on the plate. The

diameter that defines inhibition zone was then measured using a ruler. This test procedure was similarly performed for all other test samples.

Results and Discussions

Plasmonic property

Surface plasmon resonance is well known as the collective oscillation of the electrons in the conduction band when the particles absorb the electromagnetic wave [53]. Theoretically, AgNP aggregation and dispersion phenomena can be identified with the UV-vis absorption spectra. UV-vis spectra of AgNPs synthesized using different leaves extract are depicted in Fig. 1. For comparison purpose, UV–vis spectra for $AgNO_3$ solution were also included. Figs. 2a-2c show the solution color of AgNPs synthesized using *C. papaya*, *M. esculenta*, and *M. citrifolia*, respectively. It is clear that the reduction of silver ion to the formation of AgNPs in the solution occurred as indicated by the change in solution color from yellow to brown or reddish yellow to deep red (see Fig. 2).

From UV-vis spectra, the peak absorbance can be found at 485, 356, and 471 nm for AgNPs synthesized using *C. papaya*, *M. esculenta*, and *M. citrifolia*, respectively (see Fig. 3). These findings are in agreement with those found in the previous works [4, 54]. This observation has confirmed that AgNPs reduced and stabilized using different leaves extract exhibit different characteristics in their plasmonic property. Theoretically, AgNPs have spectra in the visible region ranging from 380 to 480 nm due to the excitation of localized surface Plasmon resonance [55, 56]. It is well known that their surface plasmon oscillation is extremely affected by their size, shape, and surrounding media as well as treatment employed [3, 57]. AgNPs in spherical shape can be correlated with a single peak in the UV-vis spectrum [58]. On the other hand, AgNPs in the irregular shapes have two or more peaks depending on their symmetry. The spectra characteristics exhibited in Fig. 1 suggest that AgNPs synthesized using *C. papaya*, *M. esculenta*, and *M. citrifolia* were spherical in nature.

For a comprehensive overview, AgNPs synthesized using *C. papaya* shows the highest maximum peak and followed by those using *M. esculenta* and *M. citrifolia* (see Fig. 3). The different maximum peaks of their UV-vis characteristics can be associated with the size of AgNPs. For instance, increasing the size of spherical nanoparticles from 8 to 99 nm increased their maximum peak spectra from 517 to 575 nm [59]. It was measured from the current study that the absorbance at λ_{max} of AgNPs synthesized using *C. papaya*, *M. esculenta*, and *M. citrifolia* are 1.56, 1.24, and 0.82 a.u, respectively. The different absorbance of the UV-vis spectra can be

specifically related to the agglomeration of AgNPs. The increase in the absorbance spectra indicates a higher production of AgNPs [60].

FTIR characteristics

FTIR was inspected to analyze biomolecule compounds, which can act as the capping agent for stabilizing AgNPs production. This method has previously been established and proved to be reliable [4, 61]. For this purpose, the FTIR spectra of AgNPs synthesized using different leaves extract are depicted in Fig. 4. Several prominent peaks are observed around the wave numbers ranges of 1042 to 1084 cm^{-1} (region I), 1384 to 1394 cm^{-1} (region II), 1590 to 1619 cm^{-1} (region III), and 3301 to 3444 cm^{-1} (region IV).

IR bands around 1042 to 1084 cm^{-1} are characterized as the phosphorus compounds. It was obvious in Table 2 that all leaves used in this study contained phosphorus mineral. FTIR spectra around 1384 to 1394 cm^{-1} are associated with the nitro compounds, which are reported also in AgNPs synthesized using *Cleistanthus collinus* leaves extract [62]. In addition, IR bands around 1590 to 1619 cm^{-1} are associated with the C=C stretching modes of vibration [63]. Finally, spectra peaks within 3301 to 3444 cm^{-1} are the -NH stretching modes, which were also reported by Jeyaraj et al. [61], which used *Sesbania grandiflora* leaves extract.

In region I of the wave number, AgNPs synthesized using *M. esculenta* are more intense in terms of transmittance compared to the others. The similar characteristics were also observed in region II. In region III, the transmittance of AgNPs synthesized using *C. papaya* is significantly intense compared with those nanoparticles synthesized using *M. esculenta*, and *M. citrifolia*. In the region IV, AgNPs synthesized using *M. esculenta* did not have a prominent peak. It is apparent that there were slightly different peak intensities for all synthesized AgNPs. Such difference and obvious characteristics can be correlated with the concentration of biomolecule on the surface of AgNPs [64].

Morphology and size

Morphology and size of AgNPs synthesized by chemical, physical, and biological approaches are affected by the reducing agent, stabilizer, and surrounding medium. In biological synthesis particularly that using leaves extract, their properties are extremely affected by the chemical composition of the leaves. In the present work, the shape of AgNPs synthesized using *C. papaya, M. esculenta, M. citrifolia* leaves extract is found to be spherical (see Figs. 5a-5c). It is confirmed that the single peak in the UV-vis spectra (see Fig. 1) for all synthesis solution is related to the spherical AgNPs.

Specifically, this work found that AgNP sizes synthesized using *C. papaya* were concentrated within 13 to 69 nm with an average of 40.8 nm (see Fig. 6a). In addition, AgNPs sizes synthesized using *M. esculenta* were in the range of 13 to 38 nm with an average of 23.0 nm (see Fig. 6b). For those synthesized using *M. citrifolia*, the range was 9 to 54 nm with an average of 26.5 nm (see Fig. 6c). By this procedure, the smallest AgNPs size was produced when *M. esculenta* leaves extraction was applied, followed by those extracted using *M. citrifolia* and *C. papaya*. These findings match with their previously discussed plasmonic properties.

In general, results from this study enhance the understanding of the effectiveness of the use of local leaves for synthesizing AgNPs in a purely green fashion at room temperature. It is noteworthy to see that AgNP sizes obtained using the presently employed procedure are comparable with those employing physical or mechanical treatment (see Table 1). Moreover, for certain studies such as proposed by Muthukrishnan et al. [38] and Balan et al. [35], results from this study are preferable in terms of their size. Also, the present green procedure has successfully produced AgNPs smaller than those obtained by Dipankar and Murugan [36], Prakash et al. [39], as well as the recent study by Kharat and Mendhulkar [37] and Ashraf et al. [4], who also synthesized AgNPs using leaves extract without additional treatment.

Energy dispersive characteristic

Energy dispersive X-ray spectroscopy, which is sometimes abbreviated as EDS, EDX, or XEDS is a common procedure for analyzing the basic elements on the surface of sample. Their characteristics generally depend on the source of X-ray excitation and the sample. The SEM-EDX spectra of all synthesized AgNPs can be observed in Figs. 7a-7c. The spectra characteristics have confirmed the presence of AgNPs. The sharp signal peak of the spectrum exhibits that the reduction from $AgNO_3$ to AgNPs using *C. papaya, M. esculenta,* and *M. citrifolia* were successfully carried out.

Specifically, the percentages of AgNPs synthesized using *C. papaya, M. esculenta,* and *M. citrifolia* observed in the EDX spectra are 94.69, 92.44, and 99.22%, respectively. It is ratified that AgNPs are dominant in the samples compared to other elements. The spherical AgNPs synthesized using *C. papaya* exhibit the EDX peak at approximately 3 keV. In addition, similar characteristics were also observed for those synthesized using *M. esculenta* and *M. citrifolia*. Such peaks are typical absorptions of metallic AgNPs due to the surface plasmon resonance [65]. These findings are in line with the results from previous works, which also synthesized AgNPs using leaves extract [4, 66]. The highest peaks in Figs. 3a-3c at approximately 3 keV confirm that metal AgNPs are dominant element compared to others. In addition, other smaller elemental peaks shown in Figs. 6a-6c are

possibly due to the contribution from enzymes or proteins present within *C. papaya, M. esculenta,* and *M. citrifolia* leaves. In general, this study has proven that the synthesis using different leaves extract such as *C. papaya, M. esculenta,* and *M. citrifolia* can produce AgNPs with different properties in terms of plasmonic, molecule bonding, morphology, and energy dispersive. It is well-known that the synthesis of AgNPs can be divided into three categories namely physical, chemical, and biological. In the physical approach, synthesis AgNPs using laser ablation, small ceramic heater, and thermal decomposition methods has been established. For the chemical approach, this requires three main ingredients namely a silver salt, a reducing agent, and a stabilizing or capping agent. In the biological approach, the reducing and stabilizing agents are replaced using biomolecules obtained from the living organism such as plants that are explored in this work. Proteins, enzymes, and vitamins are the biomolecules contained in the employed leaves extract (see Table 2) that can act as bioreductant from reducing metal ions to the formation of AgNPs in the solution. Moreover, the proposed purely green procedure is environmentally friendly compared to chemical or physical approach since the latter uses the chemical as reducing and stabilizing agent that may dispel toxin to the environment, in addition to their employment of huge amount of energy in the production.

Antibacterial investigation

Antibacterial activity by all leaves

Various studies had reported that *C. papaya, M. esculenta,* and *M. citrifolia* leaves extract can be used as antibacterial agents [67, 68]. Their studies confirmed that the antibacterial activity is strongly affected by the medium, extraction process, and type of bacteria. As summarized in Table 3, it can be seen that *C. papaya* inhibited bacteria colony growth of *E. coli* better than *M. esculenta* and *M. citrifolia*. These are supported by the inhibition zone observation also shown in Table 3. *C. papaya* leaves extract is able to inhibit *E. coli* growth to about 1 cm in zone diameter. Recently, *C. papaya* leaves extract was reported to act as an effective antibacterial component with the zones of inhibition in the range of 14 to 16 mm against *Staphylococcus aureus, E. coli, B. cereus,* and *Pasteurellamultocida* [67].

In inhibiting the *B. Cereus* growth, this study notices that *M. esculenta* is the most effective. It inhibits the growth of *B. Cereus* to about 1.2 cm in diameter. *M. esculenta* leaves extract can be used as an effective antibacterial against gram-positive bacteria such as *Corynebacterium diphtheriae*, *Listeria monocytogenes*, *Pseudomonas aeruginosa* and gram-negative bacteria such as *Vibrio cholera*, *Shigella flexneri*, and *Salmonella typhi* [69]. Their extract is also effective as an antibacterial against *Pseudomonas aeruginosa*, *E. coli,*

Enterobacter cloacae, *Klebsiella pneumoniae*, *Providencia stuartii*, and *Enterobacter aeorogenes* [68]. Phenolic compounds such as acubin, l-asperuloside, alizarin, and scopoletin are the chemical composition that act towards their antimicrobial activity. On the other hand, it is worthwhile to see that *M. citrifolia* did not show any antibacterial activity, a phenomenon evidenced in both colony forming and inhibition zone studies.

Antibacterial activity by synthesized AgNPs

AgNPs have been widely proven as an antibacterial and an antimicrobial agent [6, 15]. Table 4 lists the outcomes from the colony forming unit test of synthesized AgNPs against *E. coli* and *B. cereus*. It is apparent that AgNPs have completely (100%) inhibited the bacteria colonies of *E. coli* and *B. cereus* from 10^{15} initial colony to 0 colony as observed in the agar plate. In comparison, about 60×10^{1} bacterial colonies were still existed when the $AgNO_3$ solution was employed against *B. cereus* for control. In addition, the $AgNO_3$ solution also completely inhibited the colony of *E. coli*. To the best of the authors knowledge, this is the first evidence that shows that AgNPs synthesized using local plants such as *C. papaya*, *M. esculenta*, and *M. citrifolia* can act as an antibacterial agent against *E. coli* and *B. cereus*. Further proof is shown by the inhibition zone test in Table 5. It is noticed that AgNPs synthesized using *C. papaya* have inhibition zones varying from 1.8 to 2.6 cm. In addition, AgNPs synthesized using *M. esculenta* and *M. citrifolia* have inhibition zones varying from 1.7 to 2.0 cm and 1.6 to 2.2 cm, respectively. As a control, the $AgNO_3$ solution has inhibition zones about 0.7 and 1.0 cm against *E. coli* and *B. cereus*, respectively. Moreover, AgNPs synthesized using *C. papaya* show the largest average inhibition zone compared to others.

Although the mechanism of the bactericidal effect of AgNPs is still not well understood, several works provided some initial evidence that AgNPs can be used as an effective antibacterial agent. In terms of toxicity effect, the bacterial cell death was caused by the interaction between AgNPs and constituents of the bacteria membrane as a result of its structural change and the eventual damage [18]. AgNPs can be categorized as a hydrophobic material. Although they are hydrophobic, their bioaccumulation mechanism takes the role of their antibacterial properties [70]. AgNPs tend to accumulate at the bacterial membrane and further form aggregates once they are in contact with the organism. Consequently, the diminishment of the bacterial membrane integrity and its damage lead to bacteria cellular death [70]. There is also an implication that AgNPs can penetrate into the bacteria membrane [71]. Moreover, AgNPs can inhibit bacteria respiratory enzyme, which then facilitates the generation of reactive oxygen and consequently damages the cell [72]. Alternatively, the toxicity of AgNPs

is surface charge-dependent affected by the capping agent and synthesis procedure. The more negative charged AgNPs is less toxic compared with those nanoparticles having a more positive charge [64].

Conclusion

The aim of this investigation is to evaluate the effectiveness of the green procedure to synthesize AgNPs using *C. papaya*, *M. esculenta*, and *M. citrifolia* leaves extract without additional treatment such as physical or mechanical. This study has identified that the plasmonic property of AgNPs differs according to their size and reducing agent as well as stabilizing agent with AgNPs synthesized using *C. papaya* having the highest maximum peak and absorbance compared to the others. In addition, FTIR characteristics have confirmed the biomolecule bonding on AgNPs. FESEM investigations revealed that spherical AgNPs ranging from 9 to 69 nm were produced using this simple procedure. Specifically, the smallest nanoparticles can be produced when *M. esculenta* leaves were employed. Also, both leave extracts and synthesized AgNPs showed great potential as an antibacterial component against *E. coli* and *B. cereus*. In detail, *C. papaya* leaves extract was the most effective antibacterial agent against *E. coli* compared to the others. For *B. cereus*, *M. esculenta* leaves extract was the most effective to inhibit the bacteria. AgNPs synthesized using all considered leaves extract were found to completely inhibit all bacteria colonies. In addition, AgNPs synthesized using *C. papaya* showed the largest inhibition zone compared with those nanoparticles synthesized using *M. esculenta*, and *M. citrifolia.*

This work extends the knowledge for the exploration of natural resources particularly *C. papaya*, *M. esculenta*, and *M. citrifolia* as reducing and stabilizing agents for a green synthesis of AgNPs. These findings have significant implications for future medical applications particularly for providing potential antibacterial agent from natural resources and synthesized AgNPs. A further study could assess the long-term stability of AgNPs using this procedure and investigate their antibacterial performance on other bacteria.

Acknowledgements

We thank the Malaysian Ministry of Higher Education and Universiti Teknologi Malaysia for grants (R.J130000.7809.4F619 and Q.J130000.2522.14H40, respectively).

Conflict of Interest:

The authors declare that they have no conflict of interest.

359 **References**

360 1. Park M, Im J, Shin M, Min Y, Park J, Cho H, Park S, Shim M-B, Jeon S, Chung D-Y, Bae J, Park J,
361 Jeong U, Kim K (2012) Highly stretchable electric circuits from a composite material of silver
362 nanoparticles and elastomeric fibres. Nat Nanotech 7:803-809
363 2. Moore BD, Stevenson L, Watt A, Flitsch S, Turner NJ, Cassidy C, Graham D (2004) Rapid and ultra-
364 sensitive determination of enzyme activities using surface-enhanced resonance raman scattering. Nat
365 Biotechnol 22:1133-1138
366 3. Gangopadhyay P, Kesavamoorthy R, Bera S, Magudapathy P, Nair KGM, Panigrahi BK, Narasimhan
367 SV (2005) Optical absorption and photoluminescence spectroscopy of the growth of silver
368 nanoparticles. Phys Rev Lett 94:047403
369 4. Ashraf JM, Ansari MA, Khan HM, Alzohairy MA, Choi I (2016) Green synthesis of silver
370 nanoparticles and characterization of their inhibitory effects on ages formation using biophysical
371 techniques. Sci Rep 6:1-10
372 5. Nadagouda MN, Iyanna N, Lalley J, Han C, Dionysiou DD, Varma RS (2014) Synthesis of silver and
373 gold nanoparticles using antioxidants from blackberry, blueberry, pomegranate, and turmeric extracts.
374 ACS Sustainable Chem Eng 2:1717-1723
375 6. Kumar A, Vemula PK, Ajayan PM, John G (2008) Silver-nanoparticle-embedded antimicrobial paints
376 based on vegetable oil. Nat Mater 7:236-241
377 7. Atwater HA, Polman A (2010) Plasmonics for improved photovoltaic devices. Nat Mater 9:205-213
378 8. Luis López-Miranda J, Borjas-Garcia SE, Esparza R, Rosas G (2016) Synthesis and catalytic
379 evaluation of silver nanoparticles synthesized with *Aloysia triphylla* leaf extract. J Clust Sci 27:1989-
380 1999
381 9. McFarland AD, Van Duyne RP (2003) Single silver nanoparticles as real-time optical sensors with
382 zeptomole sensitivity. Nano Lett 3:1057-1062
383 10. Lee HY, Park HK, Lee YM, Kim K, Park SB (2007) A practical procedure for producing silver
384 nanocoated fabric and its antibacterial evaluation for biomedical applications. Chem Commun
385 28:2959-2961
386 11. Sharma VK, Yngard RA, Lin Y (2009) Silver nanoparticles: green synthesis and their antimicrobial
387 activities. Adv Colloid Interface Sci 145:83-96

12. Dal Lago V, Franca de Oliveira L, de Almeida Goncalves K, Kobarg J, Borba Cardoso M (2011) Size-selective silver nanoparticles: future of biomedical devices with enhanced bactericidal properties. J Mater Chem 21:12267-12273

13. Sathishkumar P, Vennila K, Jayakumar R, Yusoff ARM, Hadibarata T, Palvannan T (2016) Phyto-synthesis of silver nanoparticles using *Alternanthera tenella* leaf extract: an effective inhibitor for the migration of human breast adenocarcinoma (mcf-7) cells. Bioprocess Biosyst Eng 39:651-659

14. Guzman M, Dille J, Godet S (2012) Synthesis and antibacterial activity of silver nanoparticles against gram-positive and gram-negative bacteria. Nanomedicine 8:37-45

15. Kovács D, Igaz N, Keskeny C, Bélteky P, Tóth T, Gáspár R, Madarász D, Rázga Z, Kónya Z, Boros IM, Kiricsi M (2016) Silver nanoparticles defeat p53-positive and p53-negative osteosarcoma cells by triggering mitochondrial stress and apoptosis. Sci Rep 6:1-10

16. Agnihotri S, Mukherji S, Mukherji S (2014) Size-controlled silver nanoparticles synthesized over the range 5–100 nm using the same protocol and their antibacterial efficacy. RSC Adv 4:3974-3983

17. Raza M, Kanwal Z, Rauf A, Sabri A, Riaz S, Naseem S (2016) Size- and shape-dependent antibacterial studies of silver nanoparticles synthesized by wet chemical routes. Nanomaterials 6:1-15

18. Sondi I, Salopek-Sondi B (2004) Silver nanoparticles as antimicrobial agent: a case study on *Escherichia coli* as a model for gram-negative bacteria. J Colloid Interface Sci 275:177-182

19. Asharani PV, Yi Lian W, Zhiyuan G, Suresh V (2008) Toxicity of silver nanoparticles in zebrafish models. Nanotechnology 19:1-8

20. Braydich-Stolle L, Hussain S, Schlager JJ, Hofmann M-C (2005) In vitro cytotoxicity of nanoparticles in mammalian germline stem cells. Toxicol Sci 88:412-419

21. Hussain SM, Hess KL, Gearhart JM, Geiss KT, Schlager JJ (2005) In vitro toxicity of nanoparticles in brl 3a rat liver cells. Toxicol In Vitro 19:975-983

22. Skebo JE, Grabinski CM, Schrand AM, Schlager JJ, Hussain SM (2007) Assessment of metal nanoparticle agglomeration, uptake, and interaction using high-illuminating system. Int J Toxicol 26:135-141

23. Ramachandran R, Krishnaraj C, Sivakumar AS, Prasannakumar P, Abhay Kumar VK, Shim KS, Song C-G, Yun S-I (2017) Anticancer activity of biologically synthesized silver and gold nanoparticles on mouse myoblast cancer cells and their toxicity against embryonic zebrafish. Mater Sci Eng C Mater Biol Appl 73:674-683

418 24. Benn TM, Westerhoff P (2008) Nanoparticle silver released into water from commercially available
419 sock fabrics. Environ Sci Technol 42:4133-4139
420 25. Benn T, Cavanagh B, Hristovski K, Posner JD, Westerhoff P (2010) The release of nanosilver from
421 consumer products used in the home. J Environ Qual 39:1875-1882
422 26. Kaegi R, Voegelin A, Sinnet B, Zuleeg S, Siegrist H, Burkhardt M (2015) Transformation of AgCl
423 nanoparticles in a sewer system - a field study. Sci Total Environ 535:20-27
424 27. Kaegi R, Voegelin A, Ort C, Sinnet B, Thalmann B, Krismer J, Hagendorfer H, Elumelu M, Mueller E
425 (2013) Fate and transformation of silver nanoparticles in urban wastewater systems. Water Res
426 47:3866-3877
427 28. Sun Y, Xia Y (2002) Shape-controlled synthesis of gold and silver nanoparticles. Science 298:2176-
428 2179
429 29. Huang Z, Chen G, Zeng G, Guo Z, He K, Hu L, Wu J, Zhang L, Zhu Y, Song Z (2017) Toxicity
430 mechanisms and synergies of silver nanoparticles in 2,4-dichlorophenol degradation by *Phanerochaete*
431 *chrysosporium*. J Hazard Mater 321:37-46
432 30. Ghorashi SAA, Kamali M (2011) Synthesis of silver nanoparticles using complexing agent method:
433 Comparing the effect of ammonium hydroxide and nitric acid on some physical properties of
434 nanoparticles. J Clust Sci 22:667-672
435 31. Ajitha B, Ashok Kumar Reddy Y, Sreedhara Reddy P (2015) Green synthesis and characterization of
436 silver nanoparticles using *Lantana camara* leaf extract. Mater Sci Eng C Mater Biol Appl 49:373-381
437 32. Kumar S, Mitra A, Halder D (2017) *Centella asiatica* leaf mediated synthesis of silver nanocolloid and
438 its application as filler in gelatin based antimicrobial nanocomposite film. Food Sci Technol 75:293-
439 300
440 33. He Y, Du Z, Ma S, Cheng S, Jiang S, Liu Y, Li D, Huang H, Zhang K, Zheng X (2016) Biosynthesis,
441 antibacterial activity and anticancer effects against prostate cancer (pc-3) cells of silver nanoparticles
442 using *Dimocarpus longan* Lour. Peel extract. Nanoscale Res Lett 11:1-10
443 34. Mishra A, Tripathy SK, Yun S-I (2011) Bio-synthesis of gold and silver nanoparticles from *Candida*
444 *guilliermondii* and their antimicrobial effect against pathogenic bacteria. J Nanosci Nanotechnol
445 11:243-248

35. Balan K, Qing W, Wang Y, Liu X, Palvannan T, Wang Y, Ma F, Zhang Y (2016) Antidiabetic activity of silver nanoparticles from green synthesis using *Lonicera japonica* leaf extract. RSC Adv 6:40162-40168

36. Dipankar C, Murugan S (2012) The green synthesis, characterization and evaluation of the biological activities of silver nanoparticles synthesized from *Iresine herbstii* leaf aqueous extracts. Colloids Surf B Biointerfaces 98:112-119

37. Kharat SN, Mendhulkar VD (2016) Synthesis, characterization and studies on antioxidant activity of silver nanoparticles using *Elephantopus scaber* leaf extract. Mater Sci Eng C Mater Biol Appl 62:719-724

38. Muthukrishnan S, Bhakya S, Senthil Kumar T, Rao MV (2015) Biosynthesis, characterization and antibacterial effect of plant-mediated silver nanoparticles using *Ceropegia thwaitesii* – an endemic species. Ind Crops Prod 63:119-124

39. Prakash P, Gnanaprakasam P, Emmanuel R, Arokiyaraj S, Saravanan M (2013) Green synthesis of silver nanoparticles from leaf extract of *Mimusops elengi*, Linn. For enhanced antibacterial activity against multi drug resistant clinical isolates. Colloids Surf B Biointerfaces 108:255-259

40. Salem WM, Haridy M, Sayed WF, Hassan NH (2014) Antibacterial activity of silver nanoparticles synthesized from latex and leaf extract of *Ficus sycomorus*. Ind Crops Prod 62:228-234

41. Vijay Kumar PPN, Pammi SVN, Kollu P, Satyanarayana KVV, Shameem U (2014) Green synthesis and characterization of silver nanoparticles using *Boerhaavia diffusa* plant extract and their anti bacterial activity. Ind Crops Prod 52:562-566

42. Ferraro V, Piccirillo C, Tomlins K, Pintado ME (2016) Cassava (*Manihot esculenta* Crantz) and yam (*Dioscorea* spp.) crops and their derived foodstuffs: safety, security and nutritional value. Crit Rev Food Sci Nutr 56:2714-2727

43. Bredeson JV, Lyons JB, Prochnik SE, Wu GA, Ha CM, Edsinger-Gonzales E, Grimwood J, Schmutz J, Rabbi IY, Egesi C, Nauluvula P, Lebot V, Ndunguru J, Mkamilo G, Bart RS, Setter TL, Gleadow RM, Kulakow P, Ferguson ME, Rounsley S, Rokhsar DS (2016) Sequencing wild and cultivated cassava and related species reveals extensive interspecific hybridization and genetic diversity. Nat Biotechnol 34:562-570

44. Zin ZM, Abdul-Hamid A, Osman A (2002) Antioxidative activity of extracts from mengkudu (*Morinda citrifolia* L.) root, fruit and leaf. Food Chem 78:227-231

45. Imaga NA, Gbenle GO, Okochi VI, Adenekan S, Duro-Emmanuel T, Oyeniyi B, Dokai PN, Oyenuga M, Otumara A, Ekeh FC (2010) Phytochemical and antioxidant nutrient constituents of *Carica papaya* and *Parquetina nigrescens* extracts. Sci Res Essays 5:2201-2205

46. Nwofia GE, Ojimelukwe P, Eji C (2012) Chemical composition of leaves, fruit pulp and seeds in some *Carica papaya* (L) morphotypes. Int J Med Arom Plants 2:200-206

47. Sang S, Wang M, He K, Liu G, Dong Z, Badmaev V, Zheng QY, Ghai G, Rosen RT, Ho CT (2002) Chemical components in noni fruits and leaves (*Morinda citrifolia* L.). ACS Symp Ser 803:134-150

48. Dittmar A (1993) *Morinda citrifolia* L. use in indigenous samoan medicine. J Herbs Spices Med Plants 1:77-92

49. Chung I-M, Park I, Seung-Hyun K, Thiruvengadam M, Rajakumar G (2016) Plant-mediated synthesis of silver nanoparticles: their characteristic properties and therapeutic applications. Nanoscale Res Lett 11:1-14

50. Alsalhi MS, Devanesan S, Alfuraydi AA, Vishnubalaji R, Munusamy MA, Murugan K, Nicoletti M, Benelli G (2016) Green synthesis of silver nanoparticles using *Pimpinella anisum* seeds: antimicrobial activity and cytotoxicity on human neonatal skin stromal cells and colon cancer cells. Int J Nanomedicine 11:4439-4449

51. Mueller JH, Hinton J (1941) A protein-free medium for primary isolation of the gonococcus and meningococcus. Proc Soc Exp Biol Med 48:330-333

52. Bauer A (1966) Antibiotic susceptibility testing by a standardized single disk method. Am J Clin Pathol 45:493-496

53. Eustis S, El-Sayed MA (2006) Why gold nanoparticles are more precious than pretty gold: noble metal surface plasmon resonance and its enhancement of the radiative and nonradiative properties of nanocrystals of different shapes. Chem Soc Rev 35:209-217

54. Raveendran P, Fu J, Wallen SL (2003) Completely “green” synthesis and stabilization of metal nanoparticles. J Am Chem Soc 125:13940-13941

55. Sastry M, Mayya KS, Patil V, Paranjape DV, Hegde SG (1997) Langmuir−blodgett films of carboxylic acid derivatized silver colloidal particles: role of subphase pH on degree of cluster incorporation. J Phys Chem B 101:4954-4958

56. Sastry M, Patil V, Sainkar SR (1998) Electrostatically controlled diffusion of carboxylic acid derivatized silver colloidal particles in thermally evaporated fatty amine films. J Phys Chem B 102:1404-1410

57. Zargar M, Hamid AA, Bakar FA, Shamsudin MN, Shameli K, Jahanshiri F, Farahani F (2011) Green synthesis and antibacterial effect of silver nanoparticles using *Vitex negundo* L. Molecules 16:6667-6676

58. Shervani Z, Ikushima Y, Sato M, Kawanami H, Hakuta Y, Yokoyama T, Nagase T, Kuneida H, Aramaki K (2007) Morphology and size-controlled synthesis of silver nanoparticles in aqueous surfactant polymer solutions. Colloid Polym Sci 286:403-410

59. Link S, El-Sayed MA (1999) Size and temperature dependence of the plasmon absorption of colloidal gold nanoparticles. J Phys Chem B 103:4212-4217

60. Tan KS, Cheong KY (2013) Advances of Ag, Cu, and Ag–Cu alloy nanoparticles synthesized via chemical reduction route. J Nanopart Res 15:1-29

61. Jeyaraj M, Sathishkumar G, Sivanandhan G, MubarakAli D, Rajesh M, Arun R, Kapildev G, Manickavasagam M, Thajuddin N, Premkumar K, Ganapathi A (2013) Biogenic silver nanoparticles for cancer treatment: an experimental report. Colloids Surf B Biointerfaces 106:86-92

62. Kanipandian N, Kannan S, Ramesh R, Subramanian P, Thirumurugan R (2014) Characterization, antioxidant and cytotoxicity evaluation of green synthesized silver nanoparticles using *Cleistanthus collinus* extract as surface modifier. Mater Res Bull 49:494-502

63. Das J, Velusamy P (2013) Antibacterial effects of biosynthesized silver nanoparticles using aqueous leaf extract of *Rosmarinus officinalis* L. Mater Res Bull 48:4531-4537

64. El Badawy AM, Silva RG, Morris B, Scheckel KG, Suidan MT, Tolaymat TM (2011) Surface charge-dependent toxicity of silver nanoparticles. Environ Sci Technol 45:283-287

65. Kalathil S, Lee J, Cho MH (2011) Electrochemically active biofilm-mediated synthesis of silver nanoparticles in water. Green Chem 13:1482-1485

66. Ravichandran V, Vasanthi S, Shalini S, Ali Shah SA, Harish R (2016) Green synthesis of silver nanoparticles using *Atrocarpus altilis* leaf extract and the study of their antimicrobial and antioxidant activity. Mater Lett 180:264-267

67. Asghar N, Naqvi SAR, Hussain Z, Rasool N, Khan ZA, Shahzad SA, Sherazi TA, Janjua MRSA, Nagra SA, Zia-Ul-Haq M (2016) Compositional difference in antioxidant and antibacterial activity of all parts of the *Carica papaya* using different solvents. Chem Cent J 10:1:11

68. Noumedem JA, Mihasan M, Lacmata ST, Stefan M, Kuiate JR, Kuete V (2013) Antibacterial activities of the methanol extracts of ten cameroonian vegetables against gram-negative multidrug-resistant bacteria. BMC Complement Altern Med 13:1-9

69. Zakaria Z, Khairi H, Somchit M, Sulaiman M, Mat Jais A, Reezal I, Mat Zaid N, Abdul Wahab S, Fadzil N, Abdullah M (2006) The in vitro antibacterial activity and brine shrimp toxicity of *Manihot esculenta* var. sri pontian extracts. Int J Pharm 2:216-220

70. Le Ouay B, Stellacci F (2015) Antibacterial activity of silver nanoparticles: a surface science insight. Nano Today 10:339-354

71. Jose Ruben M, Jose Luis E, Alejandra C, Katherine H, Juan BK, Jose Tapia R, Miguel Jose Y (2005) The bactericidal effect of silver nanoparticles. Nanotechnology 16:2346-2353

72. Pal S, Tak YK, Song JM (2007) Does the antibacterial activity of silver nanoparticles depend on the shape of the nanoparticle? a study of the gram-negative bacterium *Escherichia coli*. Appl Environ Microbiol 73:1712-1720

562 **Figure Captions**

563

564 **Fig. 1.** UV-vis spectra of AgNPs synthesized by different leaves extract

565 **Fig. 2.** The solution color of AgNPs synthesized using (a) *C. papaya*, (b) *M. esculenta*, and (c) *M. citrifolia*

566 **Fig. 3.** (a) absorbance and (b) wavelength of all solutions. Note that I, II, and III refer to the $AgNO_3$+ *M.*

567 *citrifolia*, $AgNO_3$+ *M. esculenta*, and $AgNO_3$+ *C. papaya*, respectively.

568 **Fig. 4.** FTIR spectra of AgNPs synthesized using different leaves extract

569 **Fig. 5.** FESEM of AgNPs synthesized using (a) *C. papaya*, (b) *M. esculenta*, and (c) *M. citrifolia*

570 **Fig. 6.** Size distribution histograms of all synthesized AgNPs

571 **Fig. 7.** EDX spectra of AgNPs synthesized using (a) *C. papaya*, (b) *M. esculenta*, and (c) *M. citrifolia*

572

573

574

575

576

577

578

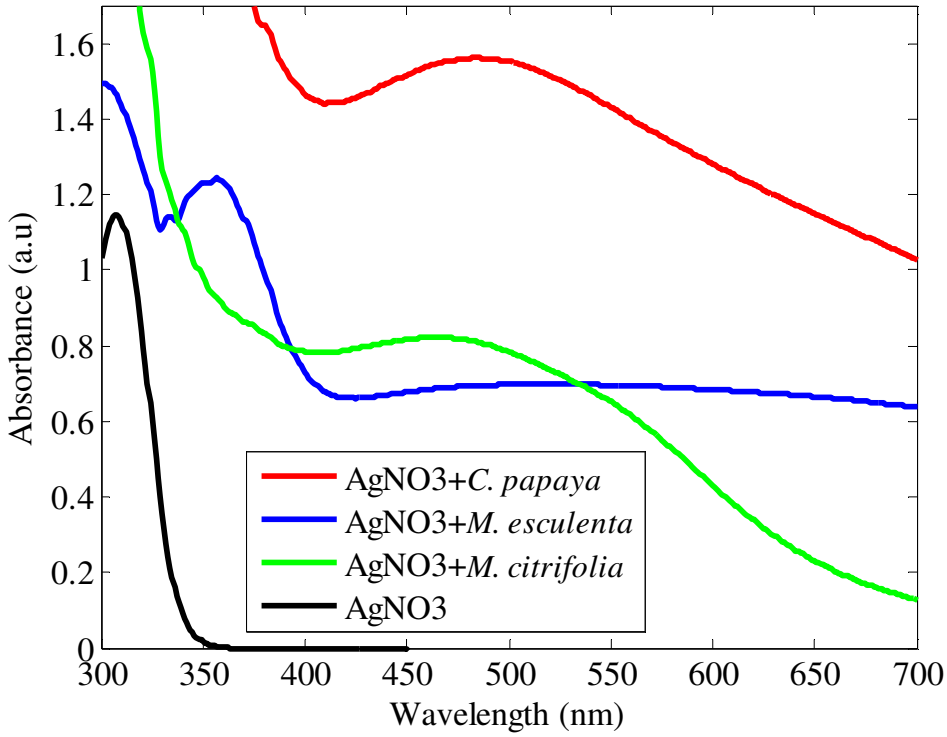

Fig. 1. UV-vis spectra of AgNPs synthesized by different leaves extract

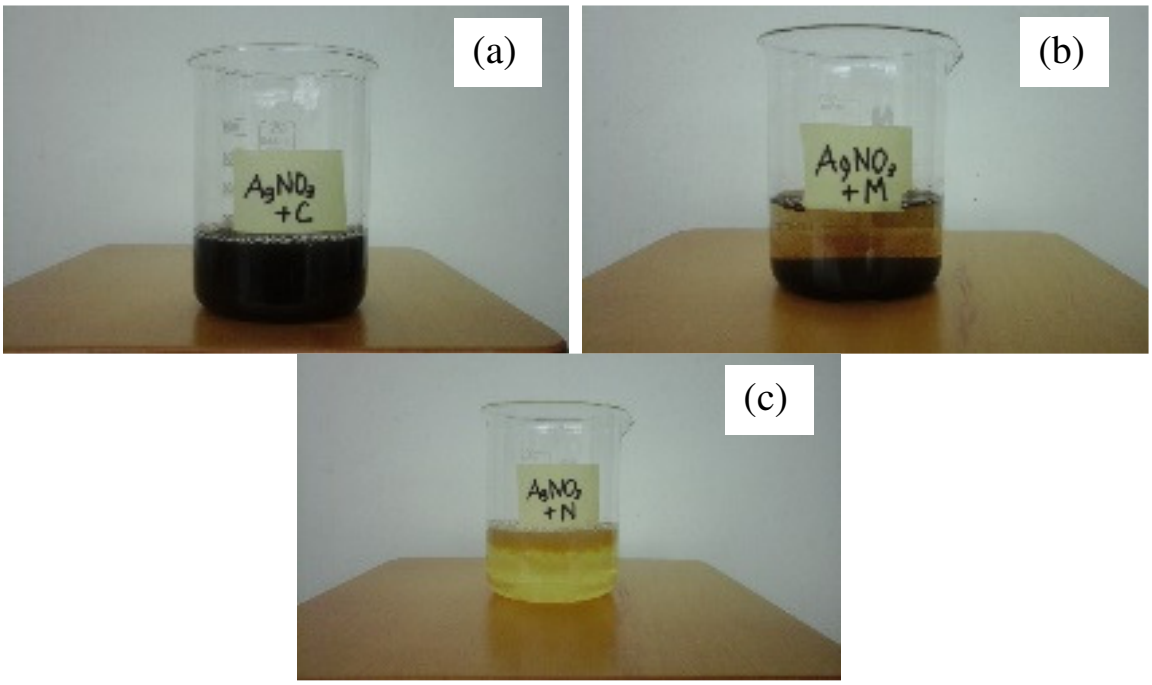

Fig. 2. The solution color of AgNPs synthesized using (a) *C. papaya*, (b) *M. esculenta*, and (c) *M. citrifolia*

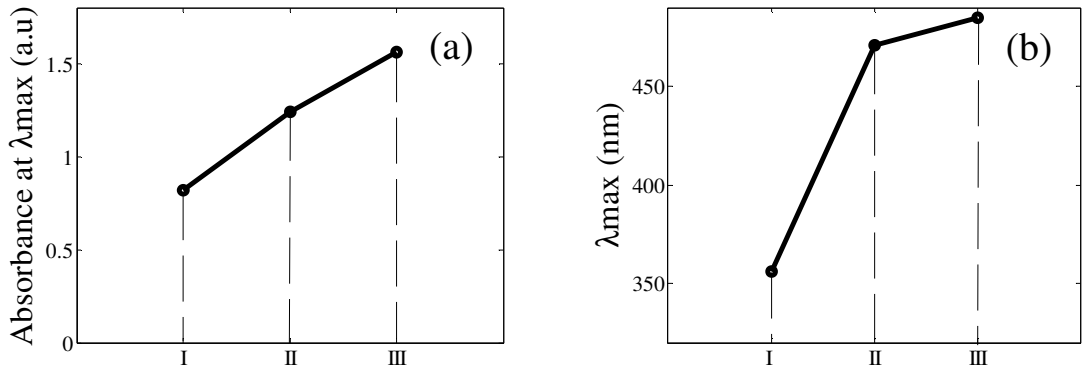

Fig. 3. (a) Absorbance and (b) wavelength of all solutions. Note that I, II, and III refer to $AgNO_3$+ *M. citrifolia*, $AgNO_3$+ *M. esculenta*, and $AgNO_3$+ *C. papaya*, respectively.

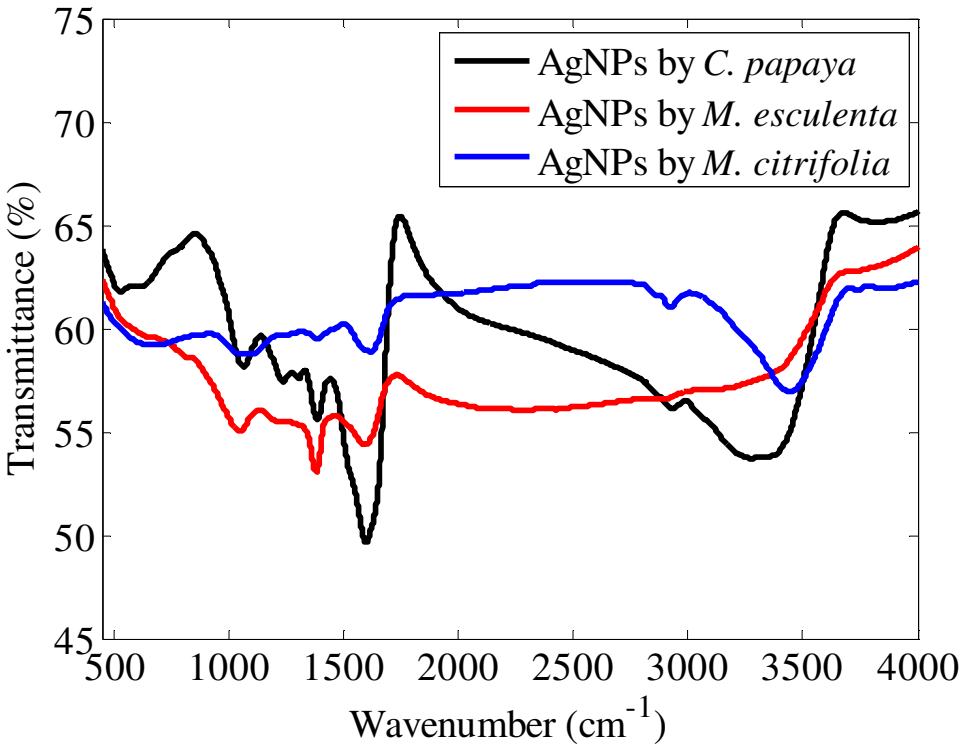

Fig. 4. FTIR spectra of AgNPs synthesized using different leaves extract

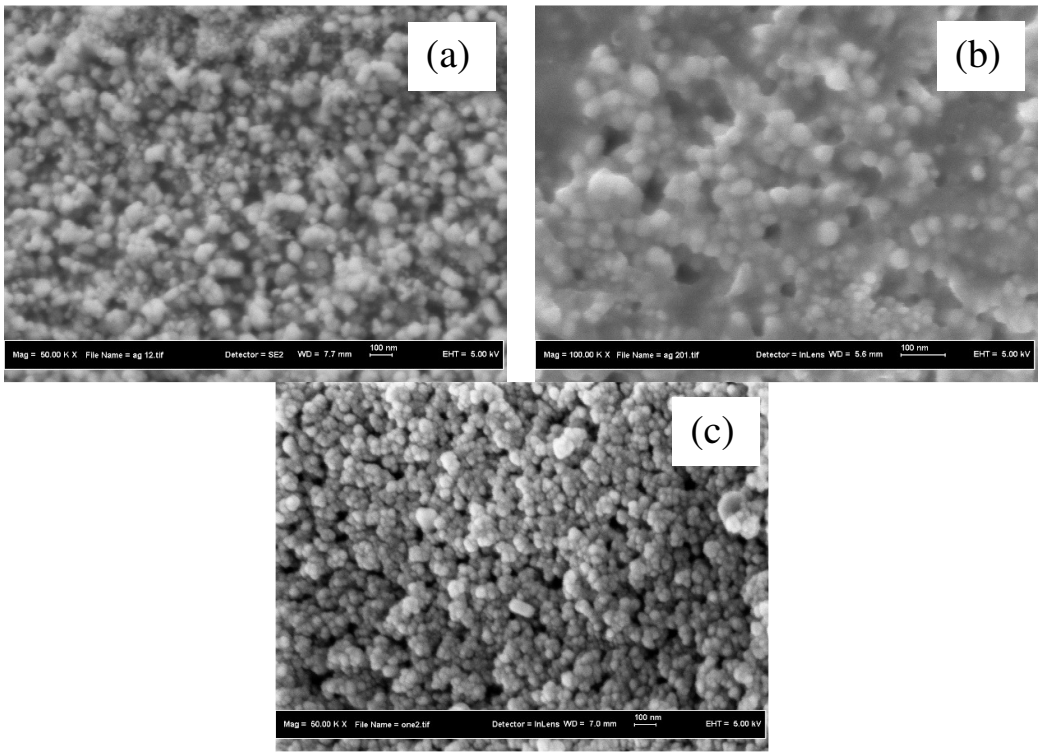

Fig. 5. FESEM of AgNPs synthesized using (a) *C. papaya*, (b) *M. esculenta*, and (c) *M. citrifolia*

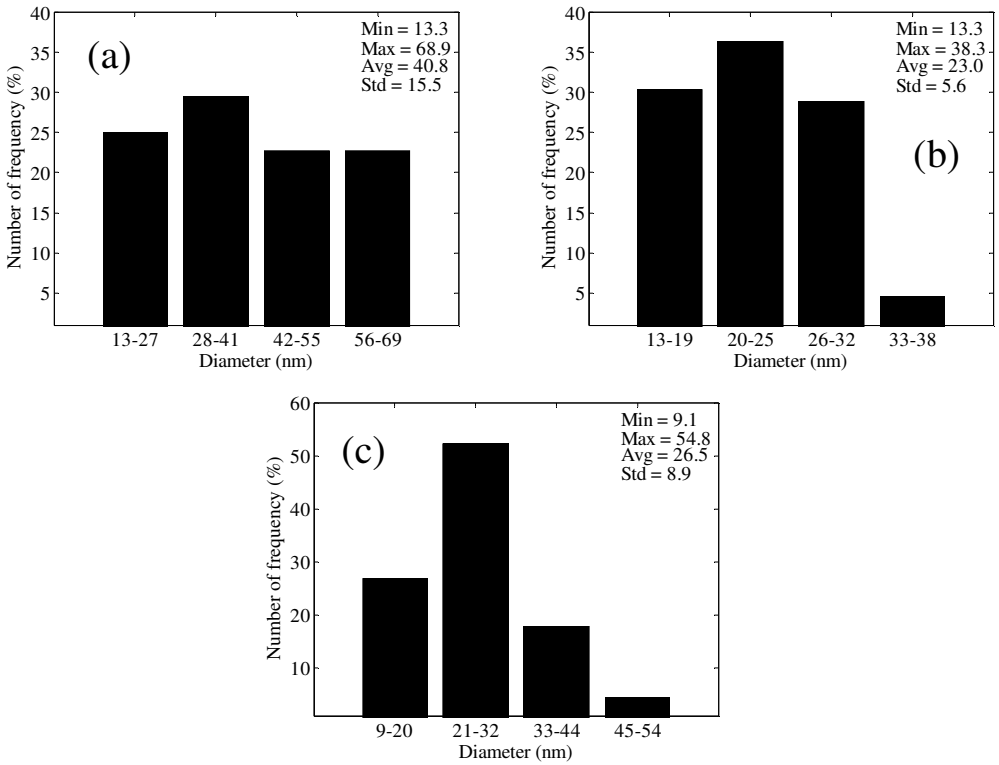

646 **Fig. 6.** Size distribution histograms of AgNPs synthesized using (a) *C. papaya*, (b) *M. esculenta*, and (c) *M.*
647 *citrifolia*

648

649

650

651

652

653

654

655

656

657

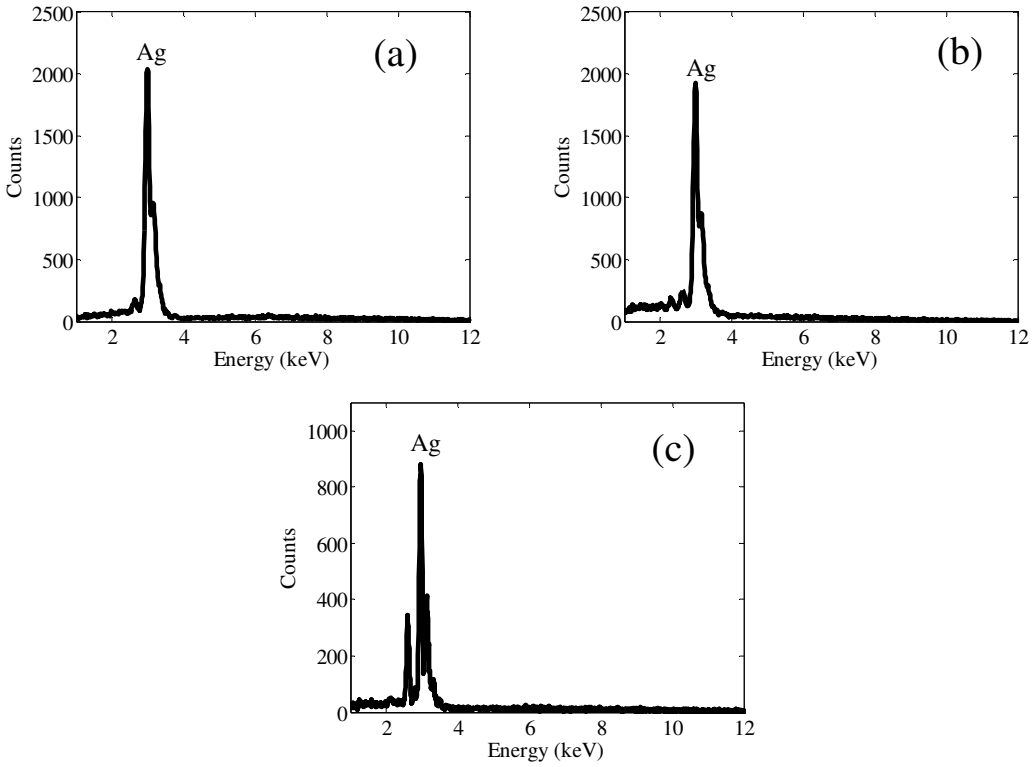

Fig. 7. EDX spectra of AgNPs synthesized using (a) *C. papaya*, (b) *M. esculenta*, and (c) *M. citrifolia*

674 **Table captions**

675 **Table 1.** Shape and size of AgNPs synthesized using various leaves extract

676 **Table 2.** Chemical compositions of *C. papaya*, *M. esculenta*, and *M. citrifolia* [42, 45-48]

677 **Table 3.** Effects of different leaves extract on the colonies and inhibition zones of *E. Coli* and *B. Cereus*

678 **Table 4.** Effects of AgNPs presence on the colonies of *E. Coli* and *B. Cereus*

679 **Table 5.** Effects of AgNPs presence on the inhibition zones of *E. Coli* and *B. Cereus*

680

681

682

683

684

685

686

687

688

689

690

691

692

693

694

695

696

697

698

699

700

701

702

703

704 **Table 1.** Shape and size of AgNPs synthesized using various leaves extract

Plant origin	Additional treatment	Silver size (nm)	References
Ficus sycomorus	Stirring and heating	1 to 20	Salem et al. [40]
Boerhaavia diffusa	Stirring and heating	25	Vijay Kumar et al. [41]
Ceropegia thwaitesii	Shaking	100	Muthukrishnan et al. [38]
Lantana camara	Stirring	14 to 34	Ajitha et al. [31]
Lonicera japonica	Heating	53	Balan et al. [35]
Centella asiatica	Stirring and heating	15	Kumar et al. [32]
Iresine herbstii	No	44 to 64	Dipankar and Murugan [36]
Mimusops elengi	No	55 to 83	Prakash et al. [39]
Aloe vera	No	5 to 85	Ashraf et al. [4]
Elephantopus scaber	No	78	Kharat and Mendhulkar [37]
Carica papaya	No	13 to 69	Present work
Manihot esculenta	No	13 to 38	Present work
Morinda citrifolia	No	9 to 54	Present work

705
706
707
708
709
710
711
712
713
714
715
716
717
718

719 **Table 2.** Chemical compositions of *C. papaya*, *M. esculenta*, and *M. citrifolia* [42, 45-48]

Leaves extract	**Proximate**	**Mineral**	**Vitamin**
C. papaya	Lipid	Calcium	Vitamin A
	Protein	Magnesium	Vitamin B12
	Crude fibre	Phosphorus	Vitamin C
	Moisture	Iron	Vitamin E
	Ash		Niacin
	Carbohydrate		Thiamine
	Fat		Riboflavin (Vitamin B2)
			Beta-carotene
M. esculenta	Caloric content	Calcium	Ascorbic acid
	Water	Copper	Niacin
	Protein	Iron	Riboflavin (Vitamin B2)
	Lipid	Magnesium	Thiamin
	Carbohydrates	Manganese	Vitamin A
	Fiber	Phosphorous	
	Ash	Potassium	
		Sodium	
M. citrifolia	Water	Calcium	Ascorbic acid
	Protein	Phosporous	Niacin
	Fat	Iron	Riboflavin (Vitamin B2)
	Carbohydrate		Thiamin
	Fiber		Beta-carotene
	Ash		

720
721
722
723
724
725
726
727
728
729
730
731

732 **Table 3.** Effects of different leaves extract on the colonies and inhibition zones of *E. Coli* and *B. Cereus*

Leaves extract	**Colony**		**Inhibition zone (cm)**	
	E. Coli	*B. Cereus*	*E. Coli*	*B. Cereus*
Carica papaya	2×10^{11}	29×10^{9}	1	0.75
Manihot esculenta	66×10^{11}	4×10^{9}	None	1.2
Morinda citrifolia	8×10^{11}	4×10^{15}	None	None

733
734
735
736
737
738
739
740
741
742
743
744
745
746
747
748
749
750
751
752
753
754
755
756

Table 4. Effects of AgNPs presence on the colonies of *E. Coli* and *B. Cereus*

Type of Leaf	***E. Coli***		***B. Cereus***	
	$AgNO_3$ + and the leaves extract (5:2)	$AgNO_3$ + and leaves extract (5:3)	$AgNO_3$ + and the leaves extract (5:2)	$AgNO_3$ + and leaves extract (5:3)
C. papaya	0	0	0	0
M. esculenta	0	0	0	0
M. citrifolia	0	0	0	0

781 **Table 5.** Effects of AgNPs presence on the inhibition zones of *E. Coli* and *B. Cereus*

Type of Leaf	***E. Coli***		***B. Cereus***	
	$AgNO_3$ + and the leaves extract (5:2)	$AgNO_3$ + and leaves extract (5:3)	$AgNO_3$ + and leaves extract (5:2)	$AgNO_3$ + and leaves extract (5:3)
C. papaya	1.8 cm	2.6 cm	1.7 cm	1.8 cm
M. esculenta	1.7 cm	2.0 cm	1.7 cm	2.0 cm
M. citrifolia	1.6 cm	2.2 cm	1.3 cm	2.4 cm

782